Chinese Chemical Letters 34 (2023) 107610

Contents lists available at ScienceDirect

Chinese Chemical Letters

journal homepage: www.elsevier.com/locate/cclet

Oxidation of diclofenac by permanganate: Kinetics, products and effect of inorganic reductants

Run Huang[a,b], Chaoting Guan[a,b,*], Qin Guo[a,b], Zhen Wang[a,b], Hanping Pan[a,b], Jin Jiang[a,b]

[a] Key Laboratory for City Cluster Environmental Safety and Green Development of the Ministry of Education, School of Ecology, Environment and Resources, Guangdong University of Technology, Guangzhou 510006, China
[b] Southern Marine Science and Engineering Guangdong Laboratory (Guangzhou), Guangzhou 511458, China

ARTICLE INFO

Article history:
Received 3 March 2022
Revised 31 May 2022
Accepted 13 June 2022
Available online 16 June 2022

Keywords:
Permanganate
Diclofenac
Aromatic secondary amines
Precursor ionization scanning
Reductant activation

ABSTRACT

The large consumption and discharge of diclofenac (DCF) lead to its frequent detection in surface water and groundwater, posing great threats to humans and ecosystems. This study explored the oxidation kinetics of DCF by permanganate (Mn(VII)), and expounded the underlying reason for the unusual pH-dependency that was unclear in previous studies. The kinetics of DCF analogues (*i.e.*, aromatic secondary amines) by Mn(VII) oxidation were comparatively investigated. Then, a tentative kinetic model involving the formation of an intermediate between Mn(VII) and DCF or its analogues was proposed to fit the pH-rate profile. Since DCF contained two chloro groups, and a carboxyl group which could be ionized by negative electrospray ionization, a precursor ionization scanning approach was used for the first time for detection of N-containing chlorinated oxidation products. New degradation pathways of DCF containing ring opening, carboxylation, carbonylation, electrophilic addition, hydroxylation and dehydrogenation were proposed based on the identified oxidation products. Moreover, it was demonstrated that the introduction of various reducing agents such as Mn(II), Fe(II) and bisulfite significantly improved the oxidation kinetics of DCF by Mn(VII). The positive effects of Mn(II) and Fe(II) were mainly attributed to the accelerated formation of MnO_2 that acted as a catalyst or co-oxidizer contributing to DCF degradation. The presence of bisulfite caused two-stage kinetics, where a sharp drop of DCF concentration followed by a slowdown of DCF removal. In the first stage, potent reactive manganese species (*e.g.*, Mn(III), Mn(V), and Mn(VI)) and sulfate radical were generated during reaction of bisulfite with Mn(VII), whereas bisulfite was depleted fast due to excess Mn(VII) concentrations and the system became the Mn(VII)/MnO_2 system in the second stage. These results provide new insight into reaction mechanism of DCF with Mn(VII) as well as propose a feasible strategy for enhancing the treatment of DCF contaminated water by Mn(VII).

Non-steroidal anti-inflammatory drugs (NSAIDs) play a pivotal role in the treatment of human and animal diseases [1]. However, due to their persistence to metabolism processes, NSAIDs may be excreted both unmetabolized and as metabolites [2]. Due to ineffective degradation in wastewater treatment processes, NSAIDs have been released into surface water and soil, leaving a host of environmental problems [3]. Diclofenac (DCF), one of the most representative NSAIDs with the highest acute toxicity, becomes one of the most prescribed drugs in the whole world for the joint pain caused by osteoarthritis [4]. The extensive production and consumption of DCF lead to its frequent detection in surface water and groundwater of different geographical regions with concentration ranging from ng/L to μg/L [5–7]. Several studies have revealed that even trace amounts of DCF, but ubiquitous in the environment, have the potential to cause adverse ecological effects [8,9]. For instance, DCF pollutants in surface water can cause exert deadly effects by damaging renal and gastrointestinal tissue in several vertebrates, such as fishes [10,11]. In addition, DCF has been reported to be associated with some human hematologic diseases, such as aplastic anemia, neutropenia, and thrombocytopenia [12]. The current researches on the removal of DCF from water sources mainly included biological treatment [13], adsorption [14], and chemical oxidation methods [15]. Among them, chemical oxidation methods that offer remarkable treatment efficiency are highly desired. However, common oxidants such as ozone (O_3), ferrate (Fe(VI)), Fenton and Fenton-like systems have some disadvantages includ-

* Corresponding author at: Key Laboratory for City Cluster Environmental Safety and Green Development of the Ministry of Education, School of Ecology, Environment and Resources, Guangdong University of Technology, Guangzhou 510006, China.
E-mail address: guanct@gdut.edu.cn (C. Guan).

https://doi.org/10.1016/j.cclet.2022.06.033
1001-8417/

ing the large amount of oxidant required, the high economic cost possible production of new pollution (*e.g.*, ferric sludges) or toxic byproducts, thus limiting their application in practical engineering processes [16,17]. Therefore, it is significant to investigate cost-effective chemical oxidation methods for the treatment of DCF contaminated water.

Permanganate (Mn(VII)), which has been widely used by water utilities to control dissolved manganese/iron irons, taste and odor compounds, has been reported to be reasonably effective in degrading some emerging micropollutants containing electron-rich moieties (*e.g.*, phenols, anilines and olefins) [18–21]. Compared with other chemical oxidants, Mn(VII) is attractive due to its comparative stability, effectiveness over a wide pH range, ease of handling, and relatively low cost [22]. Moreover, Mn(VII) is an oxidant itself and needs no extra oxidant or energy input compared to Mn-based materials, which are commonly used as catalysts for oxidation [23]. Several studies demonstrated that DCF could be oxidized fairly by Mn(VII), and the degradation kinetics of DCF decreased significantly with the increase of pH [12,24]. Similar pH dependency was observed in anilines oxidation by Mn(VII) [25]. It is noted that DCF possesses the phenylamino group in its molecular structure. However, different reasons for the pH dependency of organics oxidation by Mn(VII) were given in these studies. For instance, Cheng *et al*. proposed that amine nitrogen moiety of DCF was the most probable primary reactive site for Mn(VII) attack, and the interaction between an ionized carboxylate group and amine nitrogen might reduce the nucleophilicity of phenylamino group by inductive and resonance effects, resulting in low reactivity of the anionic DCF toward Mn(VII) [12]. Pang *et al*. proposed a kinetic model involving the formation of an intermediate between Mn(VII) and anilines to account for the pH dependency [26]. Given the contradicting explanations, the pH-dependent reaction kinetics of DCF with Mn(VII) warrant further study.

Recently, a novel precursor ionization scanning (PIS) approach using electrospray ionization-triple quadrupole mass spectrometry (ESI-QqQMS) connected with high/ultra performance liquid chromatography has been widely used for fast and selective detection of halogenated disinfection byproducts (DBPs) in water samples [27–29]. The main working principle is that polar halogen-containing compounds are collided in triple quadrupole at negative ESI to produce fragment halogen ions which can pass triple quadrupole and thus be detected [30]. Given that the PIS approach requires a negative ESI, oxidation products of N-containing organics (commonly detected in a positive ESI) are hardly detected by PIS approach. Howbeit, DCF possesses both carboxyl and halogen groups, which allows the PIS approach with a negative ESI to be used for the detection of N-containing organics.

Due to the relatively mild oxidation capacity, a high Mn(VII) dosage is needed to achieve the satisfactory removal efficiency of DCF especially under alkaline pH conditions, which however may cause the appearance of chromaticity in the treated water and also increases water treatment costs. Several studies have found that reductants can enhance organics oxidation by Mn(VII) owing to the generation of various manganese species [31–36]. For instance, it is demonstrated that colloidal MnO_2, which is formed *in situ* or *ex situ* by Mn(VII) and reductants (*e.g.*, Mn(II) and Fe(II)), could significantly accelerate the oxidation kinetics of triclosan by Mn(VII) [31,32]. In addition, some reactive manganese species (RMnS) (*i.e.*, Mn(III), Mn(V), and Mn(VI)) are formed *in situ* by Mn(VII) in the presence of reductive ligands (*e.g.*, bisulfite, pyrophosphate, EDTA, and humic acid), resulting in rapid degradation of micropollutants [31,33,35]. However, little information is available on how reductants affect the DCF oxidation by Mn(VII).

The objective of this work was to explore the underlying reason for the pH dependency of DCF oxidation by Mn(VII) and to assess the degradation performance of DCF by Mn(VII) in the presence of common reducing agents. Firstly, the reaction kinetics of Mn(VII) with DCF and its several analogues (*i.e.*, diphenylamine (DPA), 2,6-dichlorodiphenylamine (DCDPA), *N*-phenylanthranilic acid (NPAA)) were determined over a wide pH range of 4–10. The introduction of the analogues was to further understanding of the effect of carboxyl group on the pH-dependent reaction kinetics of DCF by Mn(VII). Secondly, the oxidation products of DCF reaction with Mn(VII) were identified with the HPLC/ESI-QqQMS PIS approach for the first time, and were compared with those obtained by the conventional full scan approach. Then, the tentative oxidation pathways were proposed. Finally, the promoting effect of several reductants (*i.e.*, Mn(II), Fe(II), and bisulfite) on DCF oxidation by Mn(VII) was examined.

The chemicals and materials used in the experiments were listed as follows. Diclofenac (DCF, 98%), diphenylamine (DPA, 99%), 2,6-dichlorodiphenylamine (DCDPA, 98%), *N*-phenylanthranilic acid (NPAA, 98%) were obtained from Aldrich-Sigma (detail structural formulas were shown in Table S1 in Supporting information). All the other reagents ($KMnO_4$, $MnSO_4$, $FeSO_4{\cdot}7H_2O$, CH_3COONa, $Na_2B_4O_7{\cdot}10H_2O$, NaOH, $HClO_4$, CH_3COOH) and solvents (CH_3OH) were purchased from Aldrich-Sigma, Aladdin or Sinopharm. All solutions were prepared in Milli-Q deionized water (>18 MΩ cm, Millipore). Mn(VII) stock solutions were prepared by dissolving crystal Mn(VII) in deionized water and standardized spectrophotometrically by both a direct 525 nm method and an ABTS method [32]. The stock solutions of colloidal MnO_2 were prepared following the methods reported in the literature [37] (briefly presented in Text S1 in Supporting information) and standardized by determining total manganese concentration with inductively coupled plasma optical emission spectrometer after dissolution by ascorbic acid [32]. All the experiments were conducted at 25 ± 1 °C in water bath. The change of solution pH was low (± 0.1) during the kinetic runs. All experiments were run in duplicates or triplicates, and the average data with their standard deviations were presented.

Reactions were initiated by adding Mn(VII) into pH-buffered solutions (10 mmol/L acetate buffer for pH 4–6, 10 mmol/L borax buffer for pH 7–10) containing DCF (5 μmol/L) and/or an interest constituent at desirable concentrations. Moreover, when inorganic reductants were introduced, reactions were initiated by adding desirable dosages of Mn(VII) and reductant at the same time into pH-buffered solutions containing DCF. Aliquots were periodically collected and quenched by ascorbic acid in excess and then subjected to analysis with high performance liquid chromatography (HPLC). Detail information and parameter were line in Text S2 (Supporting information).

To identify oxidation products, a series of solutions containing DCF (at a relatively high concentration of 10 μmol/L) were treated by Mn(VII) at varying doses (10–100 μmol/L) under pH 8. When the reactions reached completion (*i.e.*, Mn(VII) was totally consumed), aliquots were collected by filtration (0.2 μmol/L glass fiber filters) and analyzed by HPLC and electrospray ionization-triple quadrupole mass spectrometry (HPLC/ESI-QqQMS) using a precursor ion scan (PIS) approach (detail information and parameter were shown in Text S3 in Supporting information). The working principle for the PIS approach has been well described in literature [27–30]. Herein, the PIS of *m/z* 35 is briefly exemplified to elucidate how the PIS approach works. The mass spectrometer has three quadrupoles, Q1, Q2, and Q3 in sequence. A water sample is assumed to contain two compounds (A and B). A has chloride atoms, while B does not. These two compounds can be ionized by negative electrospray ionization to their corresponding molecular ions A^- and B^-. When these two molecular ions pass Q1 quadrupole, their *m/z* values are scanned. Then, they enter into Q2 and collide with nitrogen gas to produce fragment ions. A^- can produce chloride ion ($^{35}Cl^-$ and $^{37}Cl^-$), while B^- cannot. When the PIS of *m/z* 35 is set, only the fragment chloride ion $^{35}Cl^-$ can pass Q3

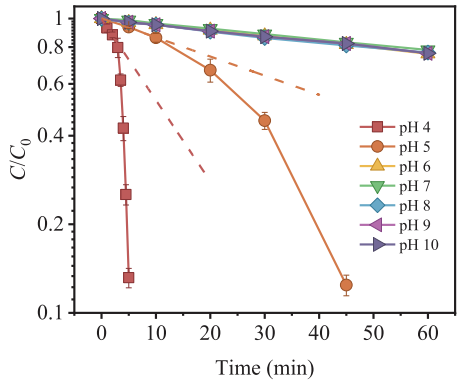

Fig. 1. Degradation of DCF by Mn(VII) oxidation. Experimental conditions: $[Mn(VII)]_0 = 50\,\mu mol/L$, $[DCF]_0 = 5\,\mu mol/L$.

and thus be detected. Meanwhile, the precursor molecular ion (*i.e.*, A^-) of $^{35}Cl^-$ is recorded and shown in the PIS spectrum of *m/z* 35. In contrast, the molecular ion B^- is silent in the PIS spectrum of *m/z* 35. Therefore, polar (*i.e.*, ionizable in negative electrospray) chloride-containing compounds in water samples can be selectively detected from the complex background matrices.

The reaction kinetics of DCF with Mn(VII) over pH 4–10 were investigated, which showed that the degradation rate of DCF decreased with pH increasing from 4 to 6, and there was no significant change of DCF degradation rate when pH was further increased to 10 (Fig. 1). The loss of DCF during Mn(VII) oxidation at pH 6–10 followed the *pseudo*-first-order kinetics (Mn(VII) was 10 times in excess than DCF), suggesting that the reaction was first-order with respect to DCF. Meanwhile, the kinetic plateau of DCF reaction with Mn(VII) could be further demonstrated by second-order rate constants ($k_{Mn(VII)}$, L mol^{-1} s^{-1}) tabulated in Table S2 in Supporting information (the calculation of $k_{Mn(VII)}$ was elaborated by Text S4 in Supporting information). Noticeably, the loss of DCF exhibited autocatalysis at pH 4–5, which was also found in Mn(VII) reaction with other organic compounds (*e.g.*, triclosan, and bromo–anilines) [25,31]. In these studies, autocatalysis was attributed to the formation of *in-situ* MnO_2 during redox reactions. To eliminate the effect of intermediate product at pH 4–5, approximated *pseudo*-first-order kinetics with the reaction rate of the initial phase (see dashed lines in Fig. 1) were utilized to determine $k_{Mn(VII)}$.

The observed pH-dependent reaction kinetics were also reported by Cheng *et al.*, where the acid-base speciation of DCF was considered as the main reason [12]. The neutral form (DCF^0) is predominant when pH < 4.2, whereas the anionic form (DCF^-) is the major form at pH > 6.0. Therefore, the ionized carboxylate group of DCF^- without the restriction of protons may interact with the amine nitrogen moiety, which can reduce the nucleophilicity of the amine nitrogen (the reactive site for Mn(VII) attack) by inductive and resonance effects. Interestingly, when we introduced the aromatic secondary amines analogues of DCF to examine the effect of carboxyl group toward the pH dependency of DCF by Mn(VII), DPA and DCDPA (without carboxyl group) both exhibited similar reaction kinetics to DCF and NPAA (with carboxyl group) (Fig. 2). This suggested that pH-dependent reaction kinetics of DCF by Mn(VII) might not be associated with the existence of carboxyl group.

Similar to DCF, the unusual pH-rate profiles were also found in our previous studies regarding the oxidation of anilines by Mn(VII), where a tentative reaction kinetic model was proposed to fit them well [26]. This model was also previously proposed by Du *et al.* and Jiang *et al.*, which well fit the pH-rate profiles of halogenated phenols (*i.e.*, chlorophenols and bromophenols) reaction with Mn(VII) [38,39]. Given DCF has the amino group similar to anilines, herein, the model (Eqs. 1–4) was attempted to fit the reaction kinetics of DCF. It was found that the model could well fit the pH-rate profiles of Mn(VII) and DCF (Fig. 2a). The detailed mathematic reasoning of kinetic equations was shown in Text S5 (Supporting information).

$$Ar_2NH_2^+ \overset{K_a}{\longleftrightarrow} H^+ + Ar_2NH \quad (1)$$

$$Mn(VII) + Ar_2NH_2^+ \overset{k_1}{\longrightarrow} \text{products} \quad (2)$$

$$Mn(VII) + Ar_2NH \underset{k_3}{\overset{k_2}{\longleftrightarrow}} Mn(VII) - Ar_2NH \quad (3)$$

$$Mn(VII) - Ar_2NH \overset{k_4}{\longrightarrow} \text{products} \quad (4)$$

In this model, undissociated amines ($Ar_2NH_2^+$) was directly oxidated with Mn(VII) while an intermediate [Mn(VII)-Ar_2NH] was formed between dissociated amines (Ar_2NH) and Mn(VII) firstly, and then [Mn(VII)-Ar_2NH] further decomposed to products. This model also well described the pH-dependent reaction kinetics of the aromatic secondary amines analogues of DCF (Figs. 2b–d, their second-order rate constants were shown in Table S2 in Supporting information). This result suggested that aromatic secondary amines had similar behaviors to DCF toward Mn(VII) oxidation, which provided additional support for the reaction mechanism between Mn(VII) and DCF.

A novel and powerful HPLC/ESI-QqQMS PIS approach, developed by Zhang's group [30], has been widely used for fast and selective detection of halogenated organics in water [39–41]. Although PIS approach required a negative ESI that was not suitable for detecting N-containing organics, DCF possessed a carboxyl group which could be ionized by negative electrospray ionization to molecular ions. Therefore, we used the PIS approach (*m/z* 35) for the detection of a sample containing DCF treated with Mn(VII) at pH 7 for comparison with the conventionally used full scan approach (Fig. 3). As could be seen, the product peaks in the chromatogram of PIS approach were much more distinct as compared to those obtained by full scan approach, which facilitated the analysis of the products and their formation pathways.

As shown in Fig. 3a, the chromatogram of oxidized DCF contained ten major product peaks as well as the peak of parent DCF. The peak at near 24 min, which was in consistent with the DCF-only case (Fig. S1 in Supporting information), showed a MS spectrum with molecular ion peaks at *m/z* 294/296 (the inset of Fig. S1 in Supporting information). Given that the isotopic abundance ratio of $^{35}Cl/^{37}Cl$ satisfies 3:1, the MS spectrum peak of DCF (containing two chlorine atoms) should correspond to the molecular ion of *m/z* 294/296. The product peaks in the chromatograms of the PIS at *m/z* 35 and 37 had the same retention times (Fig. S2 in Supporting information), suggesting that degradation products should contain Cl. The intensities of counterpart peaks at *m/z* 35 and 37 satisfied 3:1, which was further consistent with the isotopic abundance ratio of $^{35}Cl/^{37}Cl$. As shown in Fig. S3 (Supporting information), the MS spectrum of products **P1**-**P10** corresponded to two peaks (*m/z* M/M + 2), respectively, indicating that these products contained 2Cl [42]. Furthermore, the even *m/z* of main products **P1**-**P10** in negative mode indicated the presence of an odd number of N in the structure. Hence, the 2,6-dichloroaniline moiety was retained during DCF degradation, which was in accordance with the previous studies [12,24].

In addition to the products detected using the full scan approach reported in previous studies (*i.e.*, **P1**, **P3**, **P9**) [12,43,44], some previously undetected products were also found using PIS. The analysis of the ion chromatogram, corresponding MS spectrum, fragment ion patterns, and the isotopic abundance were used to

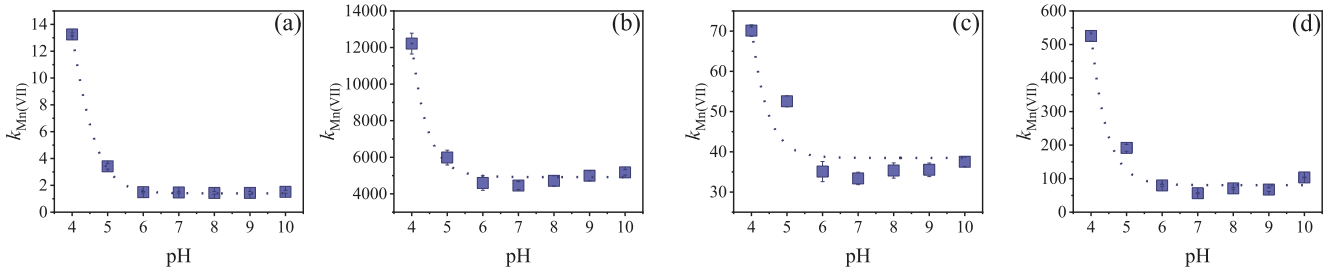

Fig. 2. Measured second-order rate constants ($k_{Mn(VII)}$, L mol^{-1} s^{-1}) of Mn(VII) reaction with four aromatic secondary amines over the pH range of 4–10. The dashed lines show the model fit. (a) DCF, (b) DPA, (c) DCDPA, and (d) NPAA.

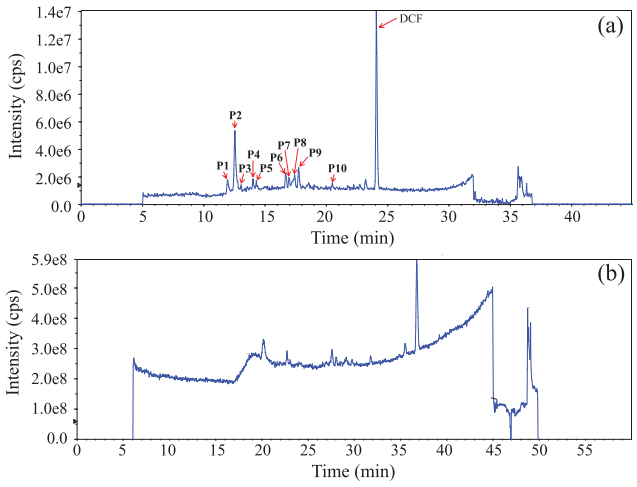

Fig. 3. LC chromatogram of DCF oxidation by Mn(VII) at pH 7 ([DCF]$_0$ = 10 μmol/L, [Mn(VII)]$_0$ = 75 μmol/L). (a) PIS approach, (b) full scan approach.

identify the molecular structure of the degradation products (Table S3 in Supporting information).

According to the analysis of main products, the degradation pathways were proposed in Fig. 4. DCF was attacked by Mn(VII) at the N–H or non-chlorinated ring site, leading to the formation of products **P2** and **P10**, respectively. The further transformation of product **P10** might undergo three different ring opening processes (pathways I, II, III). In pathway I, product **P6** was produced through the electron-richest ring opening of **P10** and formation of an aldehyde group, and it was further carbonylated to form **P4**. In pathway II, an intermediated product (IP) was tentatively proposed by the ring opening of **P10** followed by the cleavage of the C–C bond. In addition, products **P3**, **P5**, **P7**, **P9** were further generated from IP by electrophilic addition, hydroxylation, dehydrogenation. Moreover, the carboxyl groups of **P9** were formed by further oxidation of aldehyde groups. In pathway III, product **P8** was generated by the ring opening and oxidation of **P10**. Product **P1** was produced from **P8** by further cleavage of the C–C double bond and oxidation of the aldehyde groups.

As can be seen from the kinetic results, the oxidation capacity of Mn(VII) is relatively mild. Previous studies indicated that reducing agents (*e.g.*, Mn(II) and Fe(II)) could enhance the reaction of triclosan with Mn(VII) mainly attributed to the *in-situ* formed MnO_2 [31,32]. Therefore, both metal (*i.e.*, Mn(II) and Fe(II)) and non-metal (*i.e.*, bisulfite) reducing agents were introduced here to examine if the presence of reductant can enhance the removal of DCF by Mn(VII).

As shown in Fig. 5, the loss of DCF was appreciably increased owing to the presence of Mn(II) and Fe(II) under pH 5, which was attributed to the accelerated formation of MnO_2. In addition, isodose of MnO_2 (50 μmol/L) prepared *ex situ* by $Na_2S_2O_3$ and Mn(VII) was introduced as control group to further understand the role of *in situ* formed MnO_2 in the reaction of DCF by Mn(VII) oxidation (Fig. S4 in Supporting information). The *pseudo*-first-order rate constant (k_{obs}, min^{-1}) of Mn(VII)/MnO_2 under pH 5 (0.269 min^{-1}) was greater than the sum of those obtained by Mn(VII) (0.0121 min^{-1}) and MnO_2 (0.107 min^{-1}) alone oxidation, indicating that MnO_2 exhibited both oxidative and catalytic activities. Over the pH range of 5–9, Mn(II) and Fe(II) were also used to form isodose of *in-situ* MnO_2 (50 μmol/L). In particular, there was no significant difference between *in situ* and non-*in situ* MnO_2 as catalyst or oxidizer (data not shown). However, negligible influence of MnO_2 on Mn(VII) reaction with DCF under neutral/alkaline pH conditions was observed (Fig. S5 in Supporting information), indicating the weak reactivity of MnO_2 at higher pH. DCF removal by *in-situ* MnO_2 alone system was also investigated (Fig. S6 in Supporting information) for contrast, which further revealed the negligible enhancement of MnO_2 as an oxidant toward the DCF removal by Mn(VII) under neutral/alkaline pH.

When sodium bisulfite ($NaHSO_3$) was introduced as a reducing agent, the degradation of DCF exhibited two-stage kinetics, where there was a sharply drop of DCF concentration in the first stage (less than 10 s, the fastest manually sampling time) and then the rate slowed down, similar to the kinetics obtained in Mn(VII)/metal reducing agents processes (Fig. 5). This probably resulted from the generation of RMnS (*e.g.*, Mn(III), Mn(V), and Mn(VI)) and sulfate radical during reaction of bisulfite with Mn(VII) in the first stage, whereas bisulfite was depleted fast due to excess Mn(VII) concentrations and the system became the Mn(VII)/MnO_2 system in the second stage. Considerably fast reaction kinetics were also found in the degradation of other organics by the Mn(VII)/bisulfite system [45,46].

DCF degradation in the first stage showed a strong dependence on pH. The removal efficiency of DCF in this stage decreased from ~38% to ~15% as the solution pH increased from 5 to 9 (Fig. S7a in Supporting information). Meanwhile, effects of initial doses of Mn(VII) and bisulfite were also determined. As depicted in Fig. S8a (Supporting information), DCF removal efficiency in the first stage increased from ~10% to ~30% with initial dosages of Mn(VII) increasing from 50 μmol/L to 200 μmol/L and then stabilized when Mn(VII) was further increased (the ratio of Mn(VII)/bisulfite was kept at 4:3). In addition, different initial dosages of bisulfite were used at a fixed Mn(VII) dosage to clarify the effect of Mn(VII)/bisulfite ratio (from 1:0.2 to 1:20) on DCF degradation (Fig. S8b in Supporting information). Results indicated that DCF degradation in the first stage reached its maximum when Mn(VII)/bisulfite was 1:5. The degradation of the analogues of DCF were also examined in the Mn(VII)/bisulfite system over a pH range of 5–9 (Figs. S7b–d in Supporting information). Similar two-stage kinetics were also observed, suggesting the contribution of RMnS and radicals to these organics oxidation, consistent with the case of DCF.

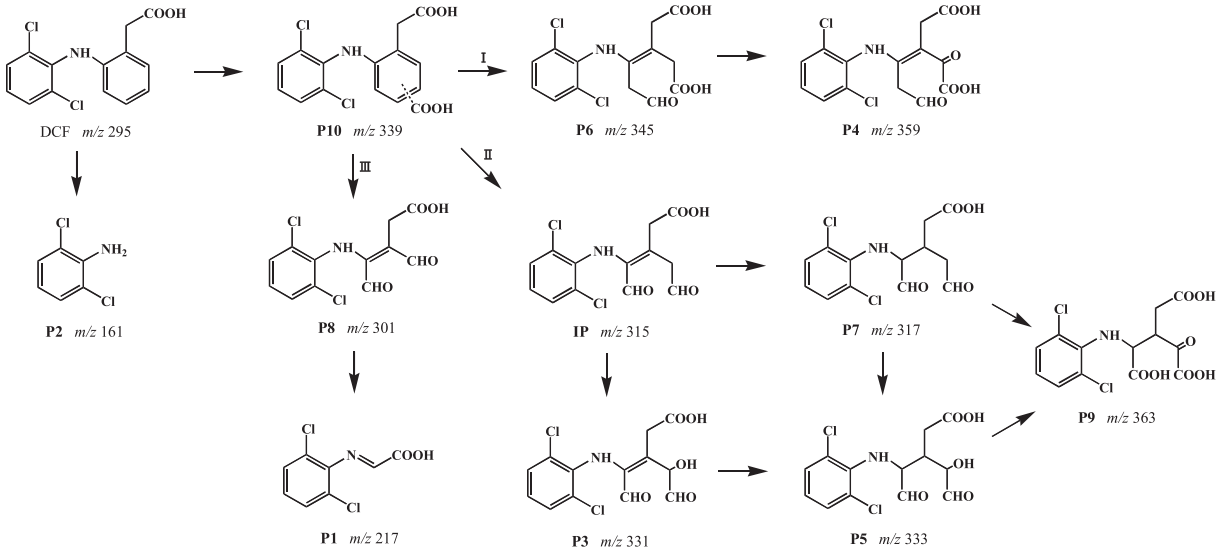

Fig. 4. Proposed degradation pathways of the DCF reaction with Mn(VII).

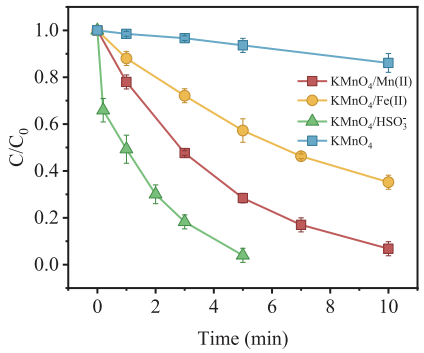

Fig. 5. The oxidation kinetics of DCF by Mn(VII) in the presence of three reduced species Mn(II), Fe(II) and $NaHSO_3$. Experimental conditions: $[DCF]_0 = 5\,\mu mol/L$, $[Mn(VII)]_0 = 70\,\mu mol/L$ with $[Mn(II)]_0 = 30\,\mu mol/L$, $[Mn(VII)]_0 = 100\,\mu mol/L$ with $[Fe(II)]_0 = 150\,\mu mol/L$, $[Mn(VII)]_0 = 100\,\mu mol/L$ with $[NaHSO_3]_0 = 75\,\mu mol/L$, $[Mn(VII)]_0 = 50\,\mu mol/L$ without reducing agent, and pH 5. (The doses of Mn(VII) and reducing agents were decided by forming both 50 μmol/L Mn(VII) and 50 μmol/L MnO_2).

In conclusion, this work investigated the pH-dependent reaction kinetics of DCF and its analogues by Mn(VII) to further understanding the potential mechanisms of aromatic secondary amines oxidation. Moreover, a PIS approach was used for the first time to analyze the oxidation products of DCF. In addition, effects of some inorganic reducing agents on DCF oxidation by Mn(VII) were evaluated. The following conclusions were obtained:

(1) The oxidation kinetics of DCF by Mn(VII) over a wide pH range of 4–10 were investigated; the second-order rate constant decreased from 13.25 L mol^{-1} s^{-1} to 1.49 L mol^{-1} s^{-1} with increasing pH from 4 to 6, and then a kinetic plateau was reached when pH was further increased to 10.
(2) A tentative kinetic model involving the formation of an intermediate between Mn(VII) and deprotonated organics was proposed, which could well fit the pH-rate profiles of DCF and its analogues reaction with Mn(VII).
(3) A novel and powerful HPLC/ESI-QqQMS PIS approach (required a negative ESI) was firstly used for the detection of degradation products of DCF, which was N-containing organics commonly detected in a positive ESI. Moreover, degradation pathways of DCF containing ring opening, carboxylation, carbonylation, electrophilic addition, hydroxylation and dehydrogenation were proposed.
(4) The introduction of various reducing agents such as Mn(II), Fe(II) and bisulfite significantly improved the oxidation kinetics of DCF by Mn(VII). Metal reductants (*i.e.*, Mn(II) and Fe(II)) could enhance DCF oxidation by Mn(VII) under acidic pH, which was mainly attributed to the accelerated formation of MnO_2. The introduction of non-metal reductant bisulfite enhanced DCF reaction with Mn(VII) over the pH range of 5–9, which showed a higher improving effects than the metal reducing agents. In the presence of bisulfite, the degradation of DCF by Mn(VII) exhibited two-stages kinetics, where a sharp drop of DCF concentration followed by a slowdown of DCF removal was observed. In the first stage, RMnS and sulfate radical were generated during reaction of bisulfite with Mn(VII) responsible for the extremely rapid oxidation of DCF, whereas bisulfite was depleted fast due to excess Mn(VII) concentrations and the system became the Mn(VII)/MnO_2 system in the second stage.

Declaration of competing interest

The authors declare that they have no known competing financial interests or personal relationships that could have appeared to influence the work reported in this paper.

Acknowledgments

This work was financially supported by the program for the National Natural Science Foundation of China (Nos. 51979044, 42177045 and 42107053), the Guangdong Natural Science Funds for Distinguished Young Scholar (No. 2019B151502023), Guangdong International Training Program for Outstanding Young Talents, the China Postdoctoral Science Foundation (No. 2021M700878), and Guangdong-Hong Kong-Macao Joint Laboratory for Contaminants Exposure and Health (No. 2020B1212030008).

Supplementary materials

Supplementary material associated with this article can be found, in the online version, at doi:10.1016/j.cclet.2022.06.033.

References

[1] L. Xu, X.Y. Cui, J.B. Liao, et al., Chin. Chem. Lett. 33 (2022) (2021) 3701–3704.

[2] J. Hofmann, U. Freier, M. Wecks, S. Hohmann, Appl. Catal. B 70 (2007) 447–451.
[3] P. Izadi, P. Izadi, R. Salem, et al., Environ. Pollut. 267 (2020) 115370.
[4] N. Vieno, M. Sillanpää, Environ. Int. 69 (2014) 28–39.
[5] E. Vulliet, C. Cren-Olive, Environ. Pollut. 159 (2011) 2929–2934.
[6] R. Lopez-Serna, A. Jurado, E. Vazquez-Sune, et al., Environ. Pollut. 174 (2013) 305–315.
[7] R.X. Ma, B. Wang, S.Y. Lu, et al., Sci. Total Environ. 557 (2016) 268–275.
[8] Y.J. Zhang, S.U. Geissen, C. Gal, Chemosphere 73 (2008) 1151–1161.
[9] L. Lonappan, S.K. Brar, R.K. Das, M. Verma, R.Y. Surampalli, Environ. Int. 96 (2016) 127–138.
[10] J. Schwaiger, H. Ferling, U. Mallow, H. Wintermayr, R.D. Negele, Aquat. Toxicol. 68 (2004) 141–150.
[11] R. Triebskorn, H. Casper, A. Heyd, et al., Aquat. Toxicol. 68 (2004) 151–166.
[12] H.Y. Cheng, D. Song, H.J. Liu, J.H. Qu, Chemosphere 136 (2015) 297–304.
[13] B. Nas, T. Dolu, M.E. Argun, et al., Sci. Total Environ. 779 (2021) 146344.
[14] C.Y. Dang, F.B. Sun, H. Jiang, et al., J. Hazard. Mater. 400 (2020) 123225.
[15] D.X. Yang, J.L. Liang, L. Luo, et al., Chin. Chem. Lett. 32 (2021) 2534–2538.
[16] S. Lim, J.L. Shi, U. von Gunten, D.L. McCurry, Water Res. 213 (2022) 118053.
[17] Z. Wang, W. Qiu, S.Y. Pang, et al., Environ. Sci. Technol. 56 (2022) 1492–1509.
[18] L.H. Hu, H.M. Martin, O. Arcs-Bulted, et al., Environ. Sci. Technol. 43 (2009) 509–515.
[19] L.H. Hu, H.M. Martin, T.J. Strathmann, Environ. Sci. Technol. 44 (2010) 6416–6422.
[20] L.H. Hu, A.M. Stemig, K.H. Wammer, T.J. Strathmann, Environ. Sci. Technol. 45 (2011) 3635–3642.
[21] J. Jiang, S.Y. Pang, J. Ma, H.L. Liu, Environ. Sci. Technol. 46 (2012) 1774–1781.
[22] J. Li, S.Y. Pang, Z. Wang, et al., Water Res. 203 (2021) 117513.
[23] F. Pan, H.D. Ji, P.H. Du, et al., J. Hazard. Mater. 402 (2021) 123779.
[24] T. Rodriguez-Alvarez, R. Rodil, J.B. Quintana, S. Trinanes, R. Cela, Water Res. 47 (2013) 3220–3230.
[25] Y. Gao, Y. Zhou, S.Y. Pang, et al., Environ. Sci. Technol. 53 (2019) 3689–3696.
[26] S.Y. Pang, J.B. Duan, Y. Zhou, Y. Gao, J. Jiang, Chemosphere 235 (2019) 104–112.
[27] F. Xiao, X.R. Zhang, H.Y. Zhai, et al., Environ. Sci. Technol. 46 (2012) 7112–7119.
[28] Y. Pan, X.R. Zhang, Environ. Sci. Technol. 47 (2013) 1265–1273.
[29] H.Y. Zhai, X.R. Zhang, X.H. Zhu, J.Q. Liu, M. Ji, Environ. Sci. Technol. 48 (2014) 2579–2588.
[30] X.R. Zhang, J.W. Talley, B. Boggess, G.Y. Ding, D. Birdsell, Environ. Sci. Technol. 42 (2008) 6598–6603.
[31] J. Jiang, S.Y. Pang, J. Ma, Environ. Sci. Technol. 43 (2009) 8326–8331.
[32] J. Jiang, Y. Gao, S.Y. Pang, et al., Environ. Sci. Technol. 49 (2015) 520–528.
[33] Y. Gao, J. Jiang, Y. Zhou, et al., Environ. Sci. Technol. 52 (2018) 4785–4793.
[34] Y.T. Zhu, J.F. Ling, L. Li, X.H. Guan, Chin. Chem. Lett. 31 (2020) 1545–1549.
[35] D.D. Rao, J. Chen, H.Y. Dong, et al., Water Res. 188 (2021) 116481.
[36] Y. Zhou, J.P. Hu, Y. Gao, et al., Chin. Chem. Lett. 33 (2022) 447–451.
[37] X.L. Huangfu, J. Jiang, J. Ma, Y.Z. Liu, J. Yang, Environ. Sci. Technol. 47 (2013) 10285–10292.
[38] J.S. Du, B. Sun, J. Zhang, G.X. Hong, Environ. Sci. Technol. 46 (2012) 8860–8867.
[39] J. Jiang, Y. Gao, S.Y. Pang, et al., Environ. Sci. Technol. 48 (2014) 10850–10858.
[40] C.T. Guan, J. Jiang, S.Y. Pang, et al., Environ. Sci. Technol. 51 (2017) 10718–10728.
[41] C.T. Guan, J. Jiang, C.W. Luo, et al., Chem. Eng. J. 337 (2018) 40–50.
[42] C.W. Luo, J. Jiang, J. Ma, et al., Water Res. 96 (2016) 12–21.
[43] Y.H. Zhu, X.X. Wang, J. Zhang, et al., Environ. Sci. Technol. 53 (2019) 9063–9072.
[44] Y.H. Zhu, C. Zhao, J.L. Liang, et al., Water Res. 165 (2019) 114975.
[45] B. Sun, X.H. Guan, J.Y. Fang, P.G. Tratnyek, Environ. Sci. Technol. 49 (2015) 12414–12421.
[46] C.T. Guan, Q. Guo, Z. Wang, et al., Water Res. 216 (2022) 118331.